

Searches for Lepton Flavour Violation and Lepton Number Violation in Hadron Decays

P. Seyfert on behalf of the LHCb Collaboration

Physikalisches Institut, Heidelberg University, Im Neuenheimer Feld 226, 69120 Heidelberg, Germany

In the Standard Model of particle physics, lepton flavour and lepton number are conserved quantities although no fundamental symmetry demands their conservation. I present recent results of searches for lepton flavour and lepton number violating hadron decays measured at the B factories and LHCb.

In addition, the LHCb collaboration has recently performed a search for the lepton flavour violating decay $\tau^- \rightarrow \mu^- \mu^- \mu^+$. The obtained upper exclusion limit, that has been presented in this talk for the first time, is of the same order of magnitude as those observed at the B factories. This is the first search for a lepton flavour violating τ decay at a hadron collider.

I. INTRODUCTION

In the Standard Model both lepton number as well as lepton flavour are conserved quantities [1, 2]. Since both can be broken in extensions of the standard model, observation of either of them would be a clear sign for new physics.

Results of the search for lepton number violation (LNV) and lepton flavour violation (LFV) in decays of hadrons are presented. These comprise the B decay modes $B^+ \rightarrow h^+ \ell^+ \ell'^-$, $B^+ \rightarrow h^- \ell^+ \ell'^+$, and the corresponding D modes $D^+ \rightarrow h^+ \ell^+ \ell'^-$ and $D^+ \rightarrow h^- \ell^+ \ell'^+$. The final state meson h may hereby either be a stable meson (pions or kaons) or in case of B decays also a D meson. Additionally to these modes, the first limit on the branching fraction $B^+ \rightarrow D^0 \pi^+ \mu^- \mu^-$ is presented as well as a new result on the search for LFV in the decay of τ leptons at the LHC.

Throughout this document charge conjugate decays are implied.

A. Lepton Number Violation

Numerous models without lepton number conservation have been proposed, see [3] for an overview. Similar to the fundamental diagram in the neutrinoless double beta decay, any neutrinoless hadron decay with two same sign leptons in the final state probes the existence of Majorana neutrinos. Of the two lowest order diagrams for LNV in meson decays, one can go through an on-shell neutrino, while the other contains a virtual neutrino (Fig. 1). In B^+ decays one of them is Cabbibo favoured depending on the final state. Thus for Majorana neutrino masses in the accessible mass range (up to 5140 MeV/ c^2) the modes $B^+ \rightarrow D^- \ell^+ \ell^+$ and $B^+ \rightarrow D^{*-} \ell^+ \ell^+$ are more sensitive and also provide a mass measurement. Beyond the accessible mass range other final states ($\pi^- \ell^+ \ell^+$, $D_s^- \ell^+ \ell^+$) are more sensitive.

In the framework of LNV through a fourth neutrino N with a large Majorana mass, an observation of LNV not only provides information about the mass m_4 of the fourth neutrino, but also on the $WN\ell$ coupling strength

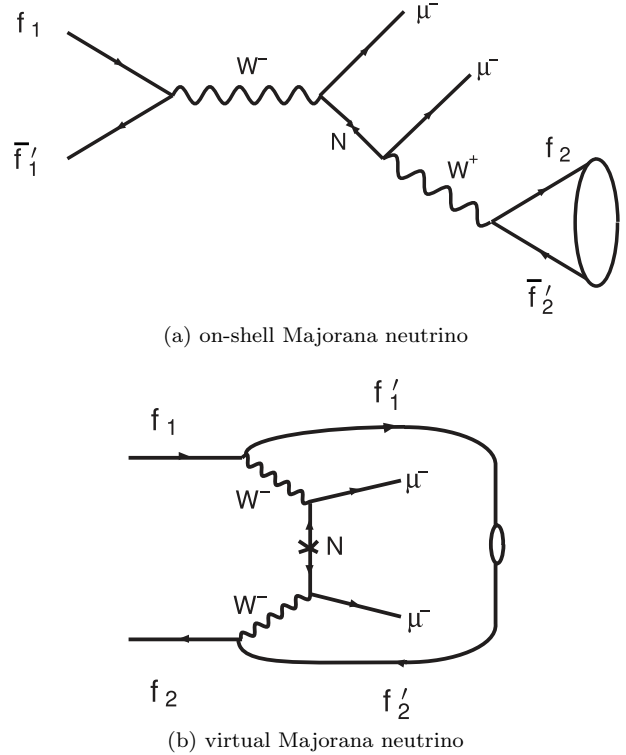
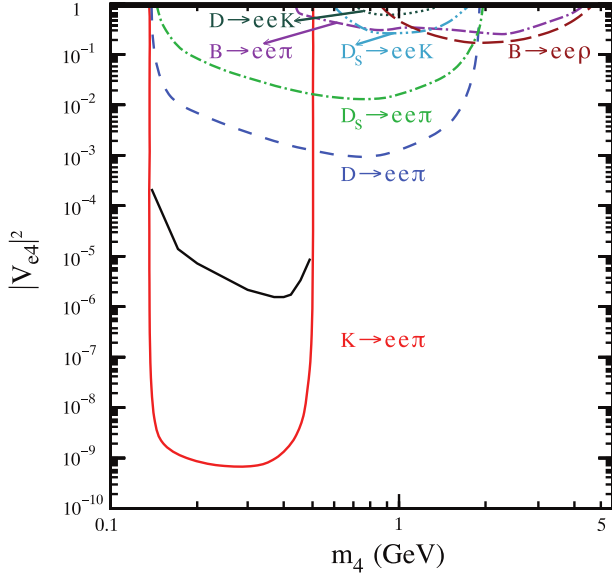


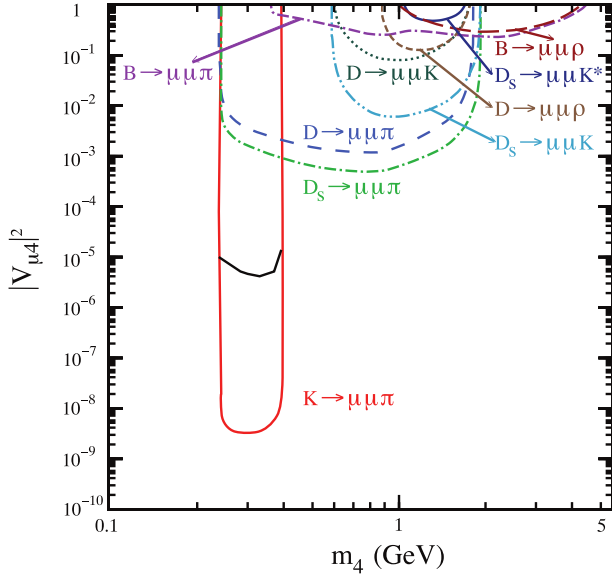
FIG. 1: Lowest order diagrams for LNV in meson decays, involving on-shell or virtual Majorana neutrinos. Depending on the individual quark flavours either of them can be Cabbibo favoured. Reproduced from [4].

$|V_{\ell 4}|$. A compilation of different exclusion limits is shown in Fig. 2. For the coupling to the muon the strongest constraints come from kaon physics.

Complementary to the modes with one meson in the final state, it has been suggested in [5] to also consider $B^+ \rightarrow D^0 \pi^+ \mu^- \mu^-$ with the diagram shown in Fig. 3. Until 2012 no limit on the branching fraction of this decay has been measured.



(a) coupling to electrons



(b) coupling to muons

FIG. 2: Constraints on charged lepton couplings V_{e4} and $V_{\mu4}$ to a fourth heavy Majorana neutrino from 2009 as a function of the mass m_4 [3].

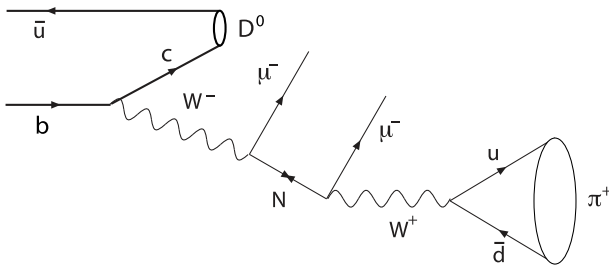


FIG. 3: Tree level Feynman diagram for the decay $B^- \rightarrow D^0 \pi^+ \mu^- \mu^-$.

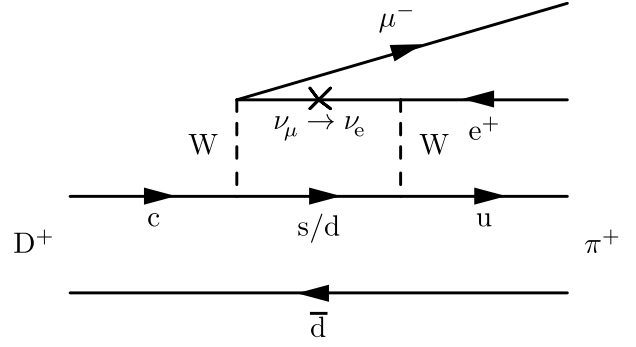


FIG. 4: Feynman diagram for lepton flavour violating meson decays in the Standard Model with neutrino oscillation.

B. Lepton Flavour Violation

In contrast to violation of lepton number, lepton flavour violation has been observed experimentally in the neutrino sector. Through loop diagrams, neutrino oscillation can also enter the charged sector as illustrated in Fig. 4 – the predicted rates however are immeasurable small, suppressed by powers of m_ν^2/m_W^2 [6].

Two examples how to introduce sizeable lepton flavour violation are multi Higgs extensions by means of new scalar particles (see e. g. [7]) as in the diagram in Fig. 5a or by means of heavy neutrinos as introduced in low scale seesaw models (e. g. [8]) which couple to electrons and muons as shown in Fig. 5b. Other ways to embed LFV in the standard model are given e. g. in [9].

Particularly interesting about LFV in B decays compared to D decays is that the B mass is high enough to produce a τ^+, μ^- pair in the final state. For new physics introduced in a Higgs coupling, this final state is most sensitive due to the high masses, and thereby Higgs couplings of the leptons involved.

Similarly the decay $\tau^- \rightarrow \mu^- \mu^- \mu^+$ is not entirely forbidden, but neutrino oscillation at loop level alone cannot bring the branching fraction to an observable level. As presented in [10] the strongest limits on LFV in lepton decays come from the $\mu^- \rightarrow e^- \gamma$ mode, the search for $\tau^- \rightarrow \mu^- \mu^- \mu^+$ is particularly interesting because some new physics models (e. g. Littlest Higgs [11]), as in Fig. 6, have enhanced lepton flavour violating couplings to heavy leptons (favouring τ over μ decays) and do not involve photon couplings and therefore enhance the three lepton final state over the $\ell \gamma$ final state [12]. Moreover to identify the character of new physics, a search in both $\ell \rightarrow \ell' \gamma$ and $\ell \rightarrow \ell' \ell' \ell'$ must be performed.

II. EXPERIMENTAL RESULTS

The study of rare decays naturally needs large event samples, which, for B and D mesons, is available at the B

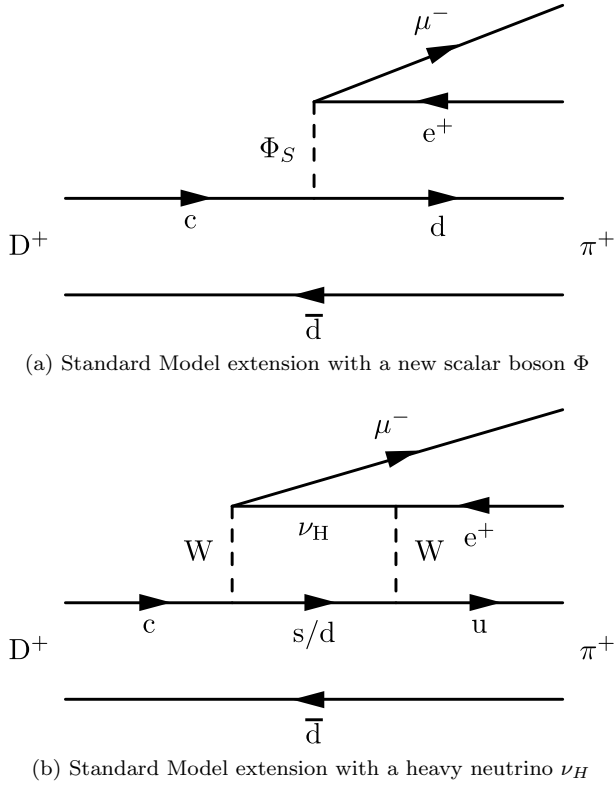


FIG. 5: Examples for introduction of lepton flavour violating in meson decays

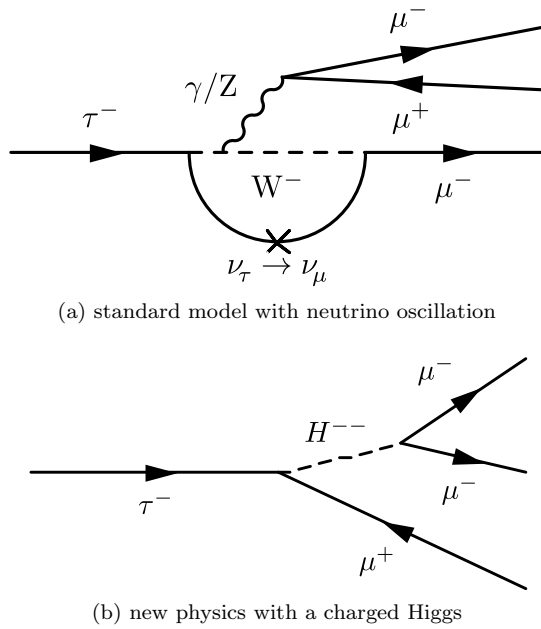


FIG. 6: Feynman diagrams for $\tau^- \rightarrow \mu^- \mu^- \mu^+$ in different models.

factories and at the LHC. The most stringent constraints on LFV and LNV in modes involving electrons come from BaBar and Belle, while muonic final states are now best constrained by recent LHCb measurements.

A. Limits on Lepton Number Violation

Decays of B^+ , D^+ , and K^+ mesons were used to search for Majorana neutrinos of different masses. The mass difference of the decaying meson and the final state lepton is the upper limit on the mass of the on-shell neutrino which can be produced. Since the neutrino mass is the invariant mass of the final state meson-lepton pair, the sum of their rest masses is the lower limit on the accessible mass range.

The strongest limits on the lepton coupling $|V_{e4}|^2$ and $|V_{\mu4}|^2$ to a fourth neutrino are in the low neutrino mass region between $140 \text{ MeV}/c^2$ and $353 \text{ MeV}/c^2$ coming from searches for the decays $K^+ \rightarrow e^+e^+\pi^-$ and $K^+ \rightarrow \mu^+\mu^+\pi^-$ respectively. Couplings down to $|V_{\ell4}|^2 \lesssim 10^{-8}$ are thereby ruled out in the most sensitive range.

The currently most stringent limits on LNV in charm decays and thereby higher neutrino masses have been obtained by the BaBar collaboration [13] shown in Tab. Ia.

The extension of the search range to higher masses is only possible in B decays, the enormous production cross section in hadron collisions makes the LHC the optimal place for searches for LNV in B decays. LHCb recently provided new results on the on-shell modes $B^+ \rightarrow \pi^- \mu^+ \mu^+$ and $B^+ \rightarrow D_s^- \mu^+ \mu^+$, as well as the virtual modes $B^+ \rightarrow D^+ \mu^+ \mu^+$ and $B^+ \rightarrow D^{*-} \mu^+ \mu^+$ [4].

Limits on the branching fraction are hereby set as a function of the neutrino mass for the on-shell modes. For comparison, assuming a flat distribution of the decay products in phase space, the observed branching fraction is shown in Tab. Ib along with the modes which are sensitive to virtual Majorana neutrinos and previous measurements.

The first search for $B^+ \rightarrow D^0 \pi^- \mu^+ \mu^+$ has been performed by LHCb [4] and showed no excess over the background. Since this channel involves an on-shell Majorana neutrino, the limit is given as a function of the neutrino mass as well.

LHCb also provides the strongest limits on $|V_{\mu4}|$ up to the B^+ mass considering these results come from $B^+ \rightarrow \pi^- \mu^+ \mu^+$, shown in Fig. 7.

A natural way to search for a lepton number violating decay is to search for same sign leptons from a common vertex. Thereby the analysis' implications on an intermediate on-shell neutrino are only drawn correctly if the lifetime of the neutrino is short enough not to degrade the reconstruction. To estimate how the observed limits are to be understood in models with long lived heavy neutrinos, LHCb also provides the relative reconstruction efficiency as a function of the neutrino lifetime, shown in Fig. 8.

TABLE I: Current limits on lepton number violating charm (a) and bottom (b) meson decays.

(a) charm decays		(b) bottom decays	
channel	limit	channel	limit
$\mathcal{B}(D^+ \rightarrow \pi^- e^+ e^+)$	$< 1.9 \times 10^{-6}$ @90 % CL [13] BaBar	$\mathcal{B}(B^- \rightarrow \pi^+ e^- e^-)$	$< 2.3 \times 10^{-8}$ @90 % CL [14] BaBar
$\mathcal{B}(D^+ \rightarrow \pi^- \mu^+ \mu^+)$	$< 2.0 \times 10^{-6}$ @90 % CL [13] BaBar	$\mathcal{B}(B^- \rightarrow K^+ e^- e^-)$	$< 3.0 \times 10^{-8}$ @90 % CL [14] BaBar
$\mathcal{B}(D^+ \rightarrow \pi^- \mu^+ e^+)$	$< 2.0 \times 10^{-6}$ @90 % CL [13] BaBar	$\mathcal{B}(B^- \rightarrow K^{*+} e^- e^-)$	$< 2.8 \times 10^{-6}$ @90 % CL [15] CLEO
$\mathcal{B}(D_s^+ \rightarrow \pi^- e^+ e^+)$	$< 4.1 \times 10^{-6}$ @90 % CL [13] BaBar	$\mathcal{B}(B^- \rightarrow \rho^+ e^- e^-)$	$< 2.6 \times 10^{-6}$ @90 % CL [15] CLEO
$\mathcal{B}(D_s^+ \rightarrow \pi^- \mu^+ \mu^+)$	$< 14 \times 10^{-6}$ @90 % CL [13] BaBar	$\mathcal{B}(B^- \rightarrow D^+ e^- e^-)$	$< 2.6 \times 10^{-6}$ @90 % CL [16] Belle
$\mathcal{B}(D_s^+ \rightarrow \pi^- \mu^+ e^+)$	$< 8.4 \times 10^{-6}$ @90 % CL [13] BaBar	$\mathcal{B}(B^- \rightarrow D^+ e^- \mu^-)$	$< 1.8 \times 10^{-6}$ @90 % CL [16] Belle
$\mathcal{B}(D^+ \rightarrow K^- e^+ e^+)$	$< 0.9 \times 10^{-6}$ @90 % CL [13] BaBar	$\mathcal{B}(B^- \rightarrow \pi^+ \mu^- \mu^-)$	$< 1.3 \times 10^{-8}$ @95 % CL [4] LHCb
$\mathcal{B}(D^+ \rightarrow K^- \mu^+ \mu^+)$	$< 10 \times 10^{-6}$ @90 % CL [13] BaBar	$\mathcal{B}(B^- \rightarrow K^+ \mu^- \mu^-)$	$< 5.4 \times 10^{-7}$ @95 % CL [17] LHCb
$\mathcal{B}(D^+ \rightarrow K^- \mu^+ e^+)$	$< 1.9 \times 10^{-6}$ @90 % CL [13] BaBar	$\mathcal{B}(B^- \rightarrow K^{*+} \mu^- \mu^-)$	$< 4.4 \times 10^{-6}$ @90 % CL [15] CLEO
$\mathcal{B}(D_s^+ \rightarrow K^- e^+ e^+)$	$< 5.2 \times 10^{-6}$ @90 % CL [13] BaBar	$\mathcal{B}(B^- \rightarrow \rho^+ \mu^- \mu^-)$	$< 5.0 \times 10^{-6}$ @90 % CL [15] CLEO
$\mathcal{B}(D_s^+ \rightarrow K^- \mu^+ \mu^+)$	$< 13 \times 10^{-6}$ @90 % CL [13] BaBar	$\mathcal{B}(B^- \rightarrow D^+ \mu^- \mu^-)$	$< 6.9 \times 10^{-7}$ @95 % CL [4] LHCb
$\mathcal{B}(D_s^+ \rightarrow K^- \mu^+ e^+)$	$< 6.1 \times 10^{-6}$ @90 % CL [13] BaBar	$\mathcal{B}(B^- \rightarrow D^{*+} \mu^- \mu^-)$	$< 2.4 \times 10^{-6}$ @95 % CL [4] LHCb
$\mathcal{B}(\Lambda_c^+ \rightarrow \bar{p} e^+ e^+)$	$< 2.7 \times 10^{-6}$ @90 % CL [13] BaBar	$\mathcal{B}(B^- \rightarrow D_s^+ \mu^- \mu^-)$	$< 5.8 \times 10^{-7}$ @95 % CL [4] LHCb
$\mathcal{B}(\Lambda_c^+ \rightarrow \bar{p} \mu^+ \mu^+)$	$< 9.4 \times 10^{-6}$ @90 % CL [13] BaBar	$\mathcal{B}(B^- \rightarrow D^0 \pi^+ \mu^- \mu^-)$	$< 1.5 \times 10^{-6}$ @95 % CL [4] LHCb
$\mathcal{B}(\Lambda_c^+ \rightarrow \bar{p} \mu^+ e^+)$	$< 16 \times 10^{-6}$ @90 % CL [13] BaBar		

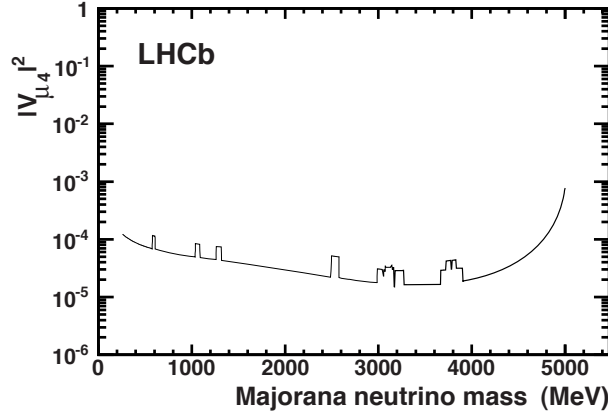
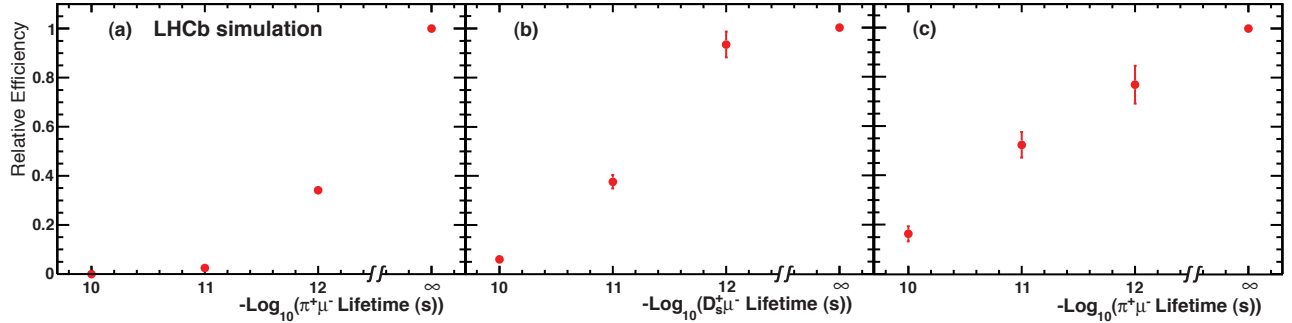
FIG. 7: Limit on $|V_{\mu 4}|^2$ from $B^- \rightarrow \pi^+ \mu^- \mu^-$ measured by LHCb [4].

FIG. 8: Relative reconstruction efficiency as a function of the Majorana neutrino lifetime. The branching fraction limits from [4] have been computed for the assumption of infinitively short lifetimes (100 % relative efficiency). For longer lifetimes, the reconstruction efficiency decreases and the observed limit has to be scaled down. The efficiencies are given for (a) $B^+ \rightarrow \pi^- \mu^+ \mu^+$, (b) $B^+ \rightarrow D_s^- \mu^+ \mu^+$, and (c) $B^+ \rightarrow D^0 \pi^- \mu^+ \mu^+$.

B. Limits on Lepton Flavour Violation

The tightest constraints on lepton flavour violating processes in charm decays have been found by the BaBar collaboration, listed in Tab. IIa. For bottom decays, Tab. IIb shows the recent results, involving τ leptons in the final state. Details are given in [18]. These results improved the limit on the energy scale at which LFV can occur [19] significantly.

The implication for new physics is that the energy scale for LFV effective operators is pushed up from 2.2 TeV to 11 TeV or from 2.6 TeV to 15 TeV for the $b \rightarrow d$ and the $b \rightarrow s$ transition respectively [19].

The most recent result in this talk is the limit on LFV in $\tau^- \rightarrow \mu^- \mu^- \mu^+$ achieved by LHCb [22]. The hadron collider environment introduces special experimental challenges compared to the B factories.

a. τ tag At the B factories, τ are produced in pairs. A clean event selection therefore is to look at events with four tracks – three from the signal candidate and one from a standard model one prong τ decay. At the LHC the main source for τ is the leptonic $D_s^- \rightarrow \tau^- \bar{\nu}_\tau$ decay [22].

b. Normalisation The τ tag automatically provides the number of produced τ which enter the analysis. Since the main production mode for τ at the LHC does not provide any further charged particles, the number of τ entering the analysis is not directly accessible. A normalisation to allowed τ decays is not possible since they are indistinguishable from more abundant D^+ decays with π^0 in the decay chain.

c. Background Having no production tag, background from events without τ , such as B and D cascade decays, is more severe in the LHCb analysis than for the B factories.

The main advantage of LHCb however is the huge production cross section for τ from D_s decays. Considering the charm and bottom production cross sections measured by LHCb [23, 24] and the known semileptonic branching fractions [25], about 8×10^{10} τ leptons have been produced at LHCb in 2011 compared to a total of 10^9 τ pairs at the B factories.

The analysis strategy of [22] is similar to other rare decay searches at LHCb. A loose cut based selection is applied to get a processable data sample. All events passing this selection are classified in a three dimensional likelihood space. The discriminating variables are the invariant mass of the $\tau^- \rightarrow \mu^- \mu^- \mu^+$ candidate, a multivariate classifier $\mathcal{M}_{3\text{body}}$ for the three body decay properties (geometry, displacement, track quality, isolation, and kinematics), and a multivariate classifier for the particle identification \mathcal{M}_{PID} (combining information from muon stations, RICH detectors, and the calorimeter signature). The latter classifiers use boosted decision trees [26] with adaptive boosting [27] as implemented by TMVA [28].

The signal efficiency of the multivariate classifiers as well as the invariant mass resolution come from

simulation and are calibrated on a control channel – $D_s^+ \rightarrow \pi^+ \phi(\mu^+ \mu^-)$ in the case for the three body classifier and the invariant mass and $B^+ \rightarrow J/\psi(\mu^+ \mu^-) K^+$ for the particle identification.

The $D_s^+ \rightarrow \phi \pi^+$ calibration channel also serves as a normalisation, since the branching fractions $\mathcal{B}(D_s^+ \rightarrow \phi \pi^+)$ and $\mathcal{B}(D_s^+ \rightarrow \tau^+ \nu_\tau)$ are known – yielding the number of τ which have been produced in D_s decays. To determine the fraction of τ from D_s decays, $f(D_s)$, the bottom and charm cross sections measured by LHCb [23, 24], as well as the branching fractions of charm and bottom hadrons to τ are used. Hereby most of the systematic uncertainties (e.g. luminosity measurement, reconstruction efficiencies) cancel, i.e. $f(D_s)$ is more accurately known than the inclusive τ production cross section. Contributions from gauge bosons or Drell-Yan processes have been evaluated to be negligible.

Using the above normalisation as well as the efficiencies for selection, reconstruction, and trigger the branching fraction can be written as follows:

$$\mathcal{B}(\tau^- \rightarrow \mu^- \mu^- \mu^+) = \frac{\mathcal{B}(D_s^+ \rightarrow \phi(\mu^+ \mu^-) \pi^+)}{\mathcal{B}(D_s^+ \rightarrow \tau^+ \nu_\tau)} \times f(D_s) \times \frac{\varepsilon_{\text{norm}}}{\varepsilon_{\text{sig}}} \frac{N_{\tau^- \rightarrow \mu^- \mu^- \mu^+}}{N_{D_s^+ \rightarrow \phi(\mu^+ \mu^-) \pi^+}}$$

where $\varepsilon_{\text{norm}}$ is the total efficiency to trigger, reconstruct and select the normalisation decay and ε_{sig} is the total efficiency for the signal channel.

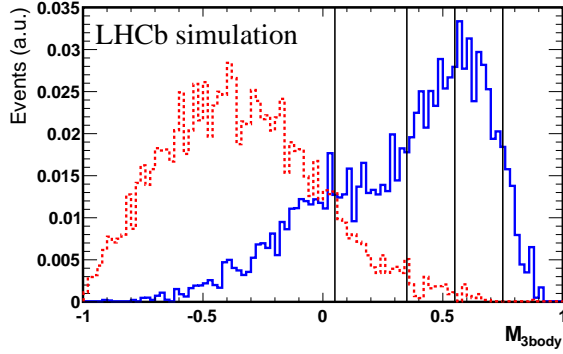
The dimuon decay of the ϕ is chosen to provide similar trigger and particle identification properties compared to the signal being sought for. The non resonant contribution from $D_s^+ \rightarrow \mu^+ \mu^- \pi^+$ decays was found to be below 2%.

The three dimensional likelihood space is subdivided into 150 bins (five for $\mathcal{M}_{3\text{body}}$ and \mathcal{M}_{PID} , and six for the invariant mass) as shown in Fig. 9 and 10a. The signal efficiency for each bin is evaluated from the calibration channels and the background in each bin is estimated from the sidebands in the invariant mass.

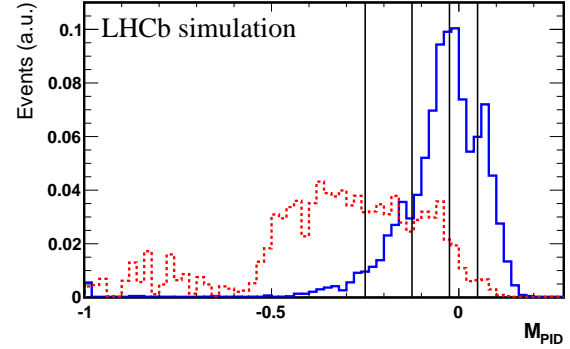
The background consists mainly of two components. Firstly combinatorial background which is modelled by an exponential and secondly by $D_s^+ \rightarrow \eta(\mu^+ \mu^- \gamma) \mu^+ \nu_\mu$ decays. This physical background is not discriminated in the current analysis by either $\mathcal{M}_{3\text{body}}$ or \mathcal{M}_{PID} as it has the same behaviour as the signal in all input quantities. Rejecting this decay will be subject of future improvements. It is modelled by an exponential multiplied by a second order polynomial for which all shape parameters have been fixed on simulated events. The normalisation is left free in the final fit within one standard deviation from the expected yield which is determined using the normalisation channel and the branching fractions $\mathcal{B}(D_s^+ \rightarrow \eta \mu^+ \nu_\mu)$, $\mathcal{B}(\eta \rightarrow \mu^+ \mu^- \gamma)$, and $\mathcal{B}(D_s^+ \rightarrow \phi \pi^+)$. For illustration the invariant mass distribution and the combined fit for the combination of the two highest $\mathcal{M}_{3\text{body}}$ and two highest \mathcal{M}_{PID} bins is shown in Fig. 10b.

TABLE II: Limits on lepton flavour violating hadron decays at 90% confidence level. All listed limits from the BaBar collaboration.

(a) charm decays		(b) bottom decays	
channel	limit	channel	limit
$\mathcal{B}(D^+ \rightarrow \pi^+ \mu^+ e^-)$	$< 3.6 \times 10^{-6}$ [13]	$\mathcal{B}(B^+ \rightarrow K^+ \tau^- \mu^+)$	$< 4.5 \times 10^{-5}$ [20]
$\mathcal{B}(D^+ \rightarrow \pi^+ e^+ \mu^-)$	$< 2.9 \times 10^{-6}$ [13]	$\mathcal{B}(B^+ \rightarrow K^+ \tau^+ \mu^-)$	$< 2.8 \times 10^{-5}$ [20]
$\mathcal{B}(D_s^+ \rightarrow \pi^+ \mu^+ e^-)$	$< 20 \times 10^{-6}$ [13]	$\mathcal{B}(B^+ \rightarrow K^+ \tau^- e^+)$	$< 4.3 \times 10^{-5}$ [20]
$\mathcal{B}(D_s^+ \rightarrow \pi^+ e^+ \mu^-)$	$< 12 \times 10^{-6}$ [13]	$\mathcal{B}(B^+ \rightarrow K^+ \tau^+ e^-)$	$< 1.5 \times 10^{-5}$ [20]
$\mathcal{B}(D^+ \rightarrow K^+ \mu^+ e^-)$	$< 2.8 \times 10^{-6}$ [13]	$\mathcal{B}(B^+ \rightarrow \pi^+ \tau^- \mu^+)$	$< 6.2 \times 10^{-5}$ [20]
$\mathcal{B}(D^+ \rightarrow K^+ e^+ \mu^-)$	$< 1.2 \times 10^{-6}$ [13]	$\mathcal{B}(B^+ \rightarrow \pi^+ \tau^+ \mu^-)$	$< 4.5 \times 10^{-5}$ [20]
$\mathcal{B}(D_s^+ \rightarrow K^+ \mu^+ e^-)$	$< 9.7 \times 10^{-6}$ [13]	$\mathcal{B}(B^+ \rightarrow \pi^+ \tau^- e^+)$	$< 7.4 \times 10^{-5}$ [20]
$\mathcal{B}(D_s^+ \rightarrow K^+ e^+ \mu^-)$	$< 14 \times 10^{-6}$ [13]	$\mathcal{B}(B^+ \rightarrow \pi^+ \tau^+ e^-)$	$< 2.0 \times 10^{-5}$ [20]
$\mathcal{B}(\Lambda_c^+ \rightarrow p \mu^+ e^-)$	$< 19 \times 10^{-6}$ [13]	$\mathcal{B}(B^+ \rightarrow \pi^+ \mu^\pm e^\mp)$	$< 1.7 \times 10^{-7}$ [21]
$\mathcal{B}(\Lambda_c^+ \rightarrow p e^+ \mu^-)$	$< 9.9 \times 10^{-6}$ [13]		



(a) Distribution for simulated background and the simulated signal as a function of the 3 body decay classifier.



(b) Distribution for simulated background and the simulated signal as a function of the PID classifier.

FIG. 9: Distribution of signal events in the two multivariate likelihoods for signal (blue / solid) and background (red / dashed).

TABLE III: Limits on the branching fraction for $\tau^- \rightarrow \mu^- \mu^- \mu^+$ obtained by different experiments.

collaboration	limit
Belle	$< 2.1 \times 10^{-8}$ @90% CL [31]
BaBar	$< 3.3 \times 10^{-8}$ @90% CL [32]
LHCb	$< 6.3 \times 10^{-8}$ @90% CL [22]

For the final limit, all bins are combined using the CLs method [29, 30]. The observed limits at 90% confidence level is 6.3×10^{-8} , in agreement with the expected limit for the absence of a signal (8.2×10^{-8}). Tab. III shows the comparison to the limits from BaBar and Belle.

III. CONCLUSION

Hadron decays measured at the B factories and at the LHC provide an excellent and abundant probe to search for LNV and LFV. So far no signal has been observed and only lower limits for the branching fractions are given. The B factories have achieved high sensitivity and ruled out branching fractions to the level of 10^{-5} . The huge production cross section of B mesons at the LHC furthermore enabled LHCb to improve the limits on LNV in B decays further. Finally, the first LFV τ decay search performed at a hadron collider has been performed.

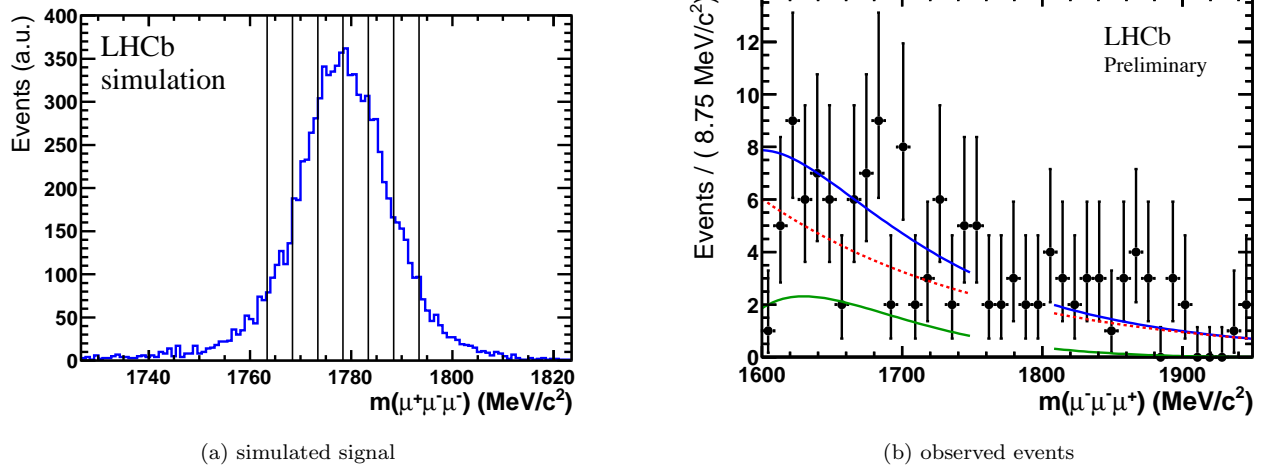


FIG. 10: Invariant mass distribution for (a) simulated signal candidates and (b) observed events in the two highest $\mathcal{M}_{\text{body}}$ and \mathcal{M}_{PID} bins. The background fit ($D_s^+ \rightarrow \eta \mu^+ \nu$ in green / dotted; combinatorial in red / dashed; combined in blue / solid) is shown in the range which is used for the fit.

-
- [1] S. Weinberg. A Model of Leptons. *Phys. Rev. Lett.*, 19:1264–1266, Nov 1967.
- [2] S. L. Glashow, J. Iliopoulos, and L. Maiani. Weak Interactions with Lepton-Hadron Symmetry. *Phys. Rev. D*, 2:1285–1292, Oct 1970.
- [3] A. Atre, T. Han, S. Pascoli, and B. Zhang. The search for heavy Majorana neutrinos. *Journal of High Energy Physics*, 2009(05):030, 2009.
- [4] R. Aaij et al. Searches for Majorana neutrinos in B^- decays. *Phys. Rev. D*, 85:112004, Jun 2012, doi:10.1103/PhysRevD.85.112004.
- [5] N. Quintero, G. Lopez Castro, and D. Delepine. Lepton number violation in top quark and neutral B meson decays. *Phys.Rev.*, D84:096011, 2011, 1108.6009.
- [6] X.-G. He, G. Valencia, and Y. Wang. Lepton flavor violating τ and b decays and heavy neutrinos. *Phys. Rev. D*, 70:113011, Dec 2004.
- [7] M. Sher and Y. Yuan. Rare b decays, rare τ decays, and grand unification. *Phys. Rev. D*, 44:1461–1472, Sep 1991.
- [8] T. Fujihara, S. K. Kang, C. S. Kim, D. Kimura, and T. Morozumi. Low scale seesaw model and lepton flavor violating rare b decays. *Phys. Rev. D*, 73:074011, Apr 2006.
- [9] S. Davidson, D. C. Bailey, and B. A. Campbell. Model independent constraints on leptoquarks from rare processes. *Z.Phys.*, C61:613–644, 1994, hep-ph/9309310.
- [10] F. Renga. Searches for LFV and LNV in charged lepton decays. In Zhao et al. [36]. FPCP2012-41.
- [11] M. Blanke, A. J. Buras, B. Duling, S. Recksiegel, and C. Tarantino. FCNC Processes in the Littlest Higgs Model with T-Parity: a 2009 Look. *Acta Phys.Polon.*, B41:657–683, 2010, 0906.5454.
- [12] M. Blanke, A. J. Buras, B. Duling, A. Poschenrieder, and C. Tarantino. Charged Lepton Flavour Violation and $(g-2)(\mu)$ in the Littlest Higgs Model with T-Parity: A Clear Distinction from Supersymmetry. *JHEP*, 0705:013, 2007, hep-ph/0702136.
- [13] J. P. Lees et al. Searches for rare or forbidden semileptonic charm decays. *Phys. Rev. D*, 84:072006, Oct 2011.
- [14] J. P. Lees et al. Search for lepton-number violating processes in $B^+ \rightarrow h^- l^+ l^+$ decays. *Phys. Rev. D*, 85:071103, Apr 2012, doi:10.1103/PhysRevD.85.071103.
- [15] K. W. Edwards et al. Search for lepton-flavor-violating decays of B mesons. *Phys. Rev. D*, 65:111102, Jun 2002, doi:10.1103/PhysRevD.65.111102.
- [16] O. Seon et al. Search for lepton-number-violating $B^+ \rightarrow D^- \ell^+ \ell'^+$ decays. *Phys. Rev. D*, 84:071106, Oct 2011, doi:10.1103/PhysRevD.84.071106.
- [17] R. Aaij et al. Search for Lepton Number Violating Decays $B^+ \rightarrow \pi^- \mu^+ \mu^+$ and $B^+ \rightarrow K^- \mu^+ \mu^+$. *Phys. Rev. Lett.*, 108:101601, Mar 2012, doi:10.1103/PhysRevLett.108.101601.
- [18] G. Marchiori. CP violation in other channels and rare decays. In Zhao et al. [36]. FPCP2012-25.
- [19] D. Black, T. Han, H.-J. He, and M. Sher. $\tau - \mu$ flavor violation as a probe of the scale of new physics. *Phys. Rev. D*, 66:053002, Sep 2002.
- [20] J. P. Lees et al. Search for the decay modes $B^\pm \rightarrow h^\pm \tau \ell$. *Phys. Rev. D*, 86:012004, Jul 2012, 1204.2852.
- [21] B. Aubert et al. Search for the Rare Decay $B \rightarrow \pi l^+ l^-$. *Phys. Rev. Lett.*, 99:051801, Jul 2007.
- [22] R. Aaij et al. Search for the lepton flavour violating decay $\tau^- \rightarrow \mu^+ \mu^- \mu^-$. May 2012. LHCb-CONF-2012-015.
- [23] Prompt charm production in pp collisions at $\sqrt{s} = 7$ TeV. Dec 2010. LHCb-CONF-2010-013.
- [24] R. Aaij et al. Measurement of b hadron production fractions in 7 TeV pp collisions. *Phys.Rev.*, D85:032008, 2012, 1111.2357.
- [25] K. Nakamura et al. Review of particle physics. *J.Phys.*, G37:075021, 2010.

- [26] L. Breiman, J. H. Friedman, R. A. Olshen, and C. J. Stone. *Classification and Regression Trees*. Wadsworth International Group, Belmont, California, 1984.
- [27] Y. Freund and R. E. Schapire. *Experiments with a new boosting algorithm*, pages 209–217. ACM Press, New York, 1996.
- [28] A. Hoecker, P. Speckmayer, J. Stelzer, J. Therhaag, E. von Toerne, and H. Voss. TMVA: Toolkit for Multivariate Data Analysis. *PoS*, ACAT:040, 2007, physics/0703039.
- [29] T. Junk. Confidence Level Computation for Combining Searches with Small Statistics. *Nucl. Instrum. Meth.*, A434:435–443, 1999, hep-ex/9902006.
- [30] A. L. Read. Presentation of search results: The CL(s) technique. *J. Phys.*, G28:2693–2704, 2002.
- [31] K. Hayasaka et al. Search for lepton-flavor-violating τ decays into three leptons with 719 million produced pairs. *Physics Letters B*, 687(23):139 – 143, 2010.
- [32] J. P. Lees et al. Limits on τ lepton-flavor violating decays into three charged leptons. *Phys. Rev. D*, 81:111101, Jun 2010.
- [33] L. J. Hall and S. Raby. Complete supersymmetric SO(10) model. *Phys. Rev. D*, 51:6524–6531, Jun 1995.
- [34] P. Fileviez Perez and M. B. Wise. Breaking Local Baryon and Lepton Number at the TeV Scale. *JHEP*, 1108:068, 2011, 1106.0343.
- [35] L. Sun. $b \rightarrow s\gamma$. In Zhao et al. [36]. FPCP2012-4.
- [36] Z.-G. Zhao, J.-X. Lu, and Q. Wang, editors. *Proceedings of the 10th International Conference on Flavor Physics and CP Violation*, 2012.
- [37] A. Zee. A theory of lepton number violation and neutrino Majorana masses. *Physics Letters B*, 93(4):389 – 393, 1980.
- [38] Y. Amhis et al. Averages of b-hadron, c-hadron, and τ -lepton properties as of early 2012. 2012, 1207.1158.